PHYSICAL REVIEW B

SOLID STATE

THIRD SERIES, VOL. 5, NO. 3 1 FEBRUARY 1972

NMR Line Narrowing by Means of Rotary Spin Echoes*

Horst Kessemeier and Won-Kyu Rhim†
Department of Physics, University of North Carolina, Chapel Hill, North Carolina
(Received 4 August 1971)

The dipolar broadened F^{19} resonance line in Teflon has been narrowed by irradiating the solid with strong continuous rf magnetic fields under magic-angle conditions. The transverse magnetization in the rotating frame lost under the action of rf and dc magnetic field inhomogeneities has been recovered by means of rotary spin echoes produced by dc magnetic field pulses. The variation of the longitudinal relaxation with direction and strength of the effective magnetic field in this compound has also been measured.

I. INTRODUCTION

The resonance response of an assembly of nuclear spins polarized in a strong dc magnetic field H_0 and interacting with each other through spin-dependent forces may, in principle, be determined to any degree of accuracy by computing the moments of the magnetic resonance absorption line. The internuclear interaction $\mathcal{H}_{\rm int}$, assumed to be small compared to the Zeeman energy, determines the shape of the free induction decay (FID) causing the signal to decay in a time T_2, the transverse relaxation time. By assumption, $\mathcal{H}_{\rm int}$ is time independent in the rigid-lattice approximation and, in general, depends on a combination of the spin operators $\vec{I}_i$ and $\vec{I}_j$ of the ith and jth nuclei, respectively, and the internuclear vector $\vec{r}_{ij}$ between them.

If $\mathcal{H}_{\rm int}$ becomes time dependent and changes in a time period of order T_2, an appropriate average of $\mathcal{H}_{\rm int}$ has to be taken resulting in a change of the FID. Two different types of time variation of $\mathcal{H}_{\rm int}$ may be distinguished: (i) $\vec{r}_{ij}$ varies rapidly with time either coherently (mechanical sample rotation[1]) or incoherently (hindered rotation or random atomic motion[2]) and (ii) the spin vectors acquire a time dependence through the application of a strong rf magnetic field H_1, which may be turned on either continuously[3–6] or in the form of a sequence of pulses spaced by time intervals of the order of or smaller than T_2.[7] In either case, any rotationally noninvariant interaction, such as the magnetic dipolar interaction $\mathcal{H}_d$ and the electric quadrupolar coupling, will be attenuated permitting the observation of smaller residual interactions in solids such as chemical shifts, Knight shifts, and the electron-coupled indirect nuclear exchange between like and unlike neighbors.[8–11]

In this paper a rotary-spin-echo (RSE) technique is introduced which reduces $\mathcal{H}_d$ and, at the same time, removes any inhomogeneity broadening caused by the dc field and, more importantly, by the rf field distributed smoothly throughout the space occupied by the sample. Lee and Goldburg[6] have calculated the second moment $\langle(\omega-\omega_e)^2\rangle$ of a dipolar broadened rotary absorption line of a spin system containing N identical particles and found

$$\langle(\omega-\omega_e)^2\rangle=\lambda_0^2(\theta)\langle(\Delta\omega)^2\rangle_{\rm LAB}+Q[\lambda_0(\theta)]/\omega_e^2 . \quad (1)$$

Here $\langle(\Delta\omega)^2\rangle_{\rm LAB}$ is the second moment of the nuclear absorption line in the laboratory frame, $\lambda_0(\theta)=\frac{1}{2}\times(3\cos^2\theta-1)$, with θ being the angle between H_0 and the effective magnetic field $H_e=\omega_e/\gamma=[(H_0-\omega/\gamma)^2+H_1^2]^{1/2}$ in the rotating frame, and $Q[\lambda_0(\theta)]$ is the contribution of the nonsecular part of $\mathcal{H}_d$.

The contribution of the secular part of $\mathcal{H}_d$ to the second moment in the rotating frame is thus reduced by a factor of $\lambda_0^2(\theta)$. At the magic angle defined by $\lambda_0(\theta)=0$, the secular-term contribution vanishes and the second moment is inversely proportional to ω_e^2, allowing for the possibility of reducing $\langle(\omega-\omega_e)^2\rangle$ indefinitely by simply increasing ω_e. For a finite ω_e, the rate of decay of any component of magnetization perpendicular to H_e is determined by the nonsecular terms as long as spin-lattice relaxation effects may be ignored. Large ω_e are obtained experimentally by applying rf pulses with large H_1; however, the inhomogeneity of H_1 is typically proportional to H_1 itself. Therefore, particularly at the magic angle, the nonsecular-

term contribution will finally be screened by rf inhomogeneity effects as H_1 increases. At this point the line can be narrowed further only by generating RSE's.

RSE's may be obtained by either phase inverting $\vec{H}_e$ or by flipping the dephased magnetization vectors through 180° in the rotating frame in a time small compared to $1/\omega_e$ analogously to producing spin echoes in the laboratory frame by applying a 90°–180° pulse sequence. We have chosen the second approach for its experimental simplicity.

In Sec. II, the influence of magnetic field inhomogeneities on the rotary FID's and their cancellation is being investigated theoretically. The experimental results are reported and discussed in Sec. III. Section IV contains a summary of this investigation.

II. THEORETICAL CONSIDERATIONS

A calculation concerning the feasibility of removing all inhomogeneities of the effective field H_e by means of suitable pulse combinations involves a transformation of the internuclear couplings from the laboratory frame (x, y, z) to the tilted rotating frame (X, Y, Z). Although such a procedure has been described repeatedly in the literature,[3,12] it must be outlined here from the point of view that the dc and rf magnetic fields are not homogeneous across the sample.

Consider a sample composed of N particles each having spin $\vec{I}$ and gyromagnetic ratio γ. It is exposed to a magnetic field

$$\vec{H} = \vec{H}_0 + 2\vec{H}_1 \cos\omega t \,, \tag{2}$$

which may vary in magnitude and direction over the sample. The laboratory coordinate system is chosen such that the z axis is in the direction of the average value of $\vec{H}_0$ experienced by the spins, and the average value of $\vec{H}_1$ may be assumed to be in the xz plane without loss of generality. Then

$$\vec{H}_0 = \Delta H_{0x}\hat{x} + \Delta H_{0y}\hat{y} + (\langle H_0\rangle + \Delta H_{0z})\hat{z} \tag{3}$$

and

$$\vec{H}_1 = (\langle H_{1x}\rangle + \Delta H_{1x})\hat{x} + \Delta H_{1y}\hat{y} + (\langle H_{1z}\rangle + \Delta H_{1z})\hat{z} \,,$$

where the average values $\langle \Delta H_{0x}\rangle = \langle \Delta H_{0y}\rangle = \langle \Delta H_{0z}\rangle = 0$; $\langle \Delta H_{1x}\rangle = \langle \Delta H_{1y}\rangle = \langle \Delta H_{1z}\rangle = 0$. It should be noted that $\langle H_{1x}\rangle$ is large compared to $\langle H_{1z}\rangle$ and to all the components of $\Delta\vec{H}_0$ and $\Delta\vec{H}_1$ under present experimental conditions.

The Hamiltonian of the spin system in the laboratory frame is given by

$$\mathcal{H} = \hbar[-\gamma(\vec{H}_0 + 2\vec{H}_1\cos\omega t)\cdot\vec{I} + \mathcal{H}_c + \mathcal{H}_0] \,, \tag{4}$$

where $\mathcal{H}_c = \sum_i \delta_i I_{zi}$ denotes the chemical-shift Hamiltonian with chemical-shift constant δ_i for the ith spin, and

$$\mathcal{H}_0 = \sum_{i<j} B_{ij}(I_{zi}I_{zj} - \tfrac{1}{3}\vec{I}_i\cdot\vec{I}_j),$$

where

$$B_{ij} = \tfrac{3}{2}\gamma^2\hbar(1 - 3\cos^2\theta_{ij})/r_{ij}^3$$

is the secular part of the dipolar interaction. The total Hamiltonian considered here then becomes

$$\begin{aligned}\mathcal{H} = \hbar\{&-\langle\omega_0\rangle I_z - 2(\langle\omega_{1x}\rangle I_x + \langle\omega_{1z}\rangle I_z)\cos\omega t \\ &- \textstyle\sum_k[(\Delta\omega_{0x})_k I_{xk} + (\Delta\omega_{0y})_k I_{yk} + (\Delta\omega_{0z})_k I_{zk}] \\ &- 2\textstyle\sum_k[(\Delta\omega_{1x})_k I_{xk} + (\Delta\omega_{1y})_k I_{yk} \\ &+ (\Delta\omega_{1z})_k I_{zk}]\cos\omega t + \mathcal{H}_c + \mathcal{H}_0\},\end{aligned} \tag{5}$$

where $\langle\omega_0\rangle = \gamma\langle H_0\rangle$, $\langle\omega_{1x}\rangle = \gamma\langle H_{1x}\rangle$, $(\Delta\omega_{0x})_k = \gamma(\Delta H_{0x})_k$, $(\Delta\omega_{1x})_k = \gamma(\Delta H_{1x})_k$, and similarly for the y and z components.

We now perform a transformation to a rotating-coordinate system in which $\langle H_{1x}\rangle$ is static. The Hamiltonian in this first rotating frame is defined by

$$\mathcal{H}_{er} = e^{-i\omega t I_z}(\mathcal{H} + \hbar\omega I_z)e^{i\omega t I_z} \,, \tag{6}$$

or, with (5),

$$\begin{aligned}\mathcal{H}_{er} = \hbar\{&-(\langle\omega_0\rangle - \omega)I_z - \langle\omega_1\rangle I_x - \textstyle\sum_k(\Delta\omega_{0z})_k I_{zk} \\ &- \textstyle\sum_k[(\Delta\omega_{1x})_k I_{xk} + (\Delta\omega_{1y})_k I_{yk}] + \mathcal{H}_c + \mathcal{H}_0\},\end{aligned} \tag{7}$$

where the time-dependent terms have been omitted since they produce no observable effects under typical experimental conditions.[3] Hence, in the rotating-coordinate frame, there is an effective magnetic field

$$\vec{H}_e = [(\langle\omega_0\rangle - \omega)\hat{z} + \langle\omega_1\rangle\hat{x}]/\gamma \equiv \vec{\omega}_e/\gamma \,, \tag{8}$$

which makes an angle

$$\theta = \arctan|\langle\omega_1\rangle/(\langle\omega_0\rangle - \omega)| \tag{9}$$

with the z axis.

Consider now the following unitary transformation of $\mathcal{H}_{er}$ to a tilted frame by the angle θ of Eq. (9) around the y axis such that $\vec{H}_e$ is parallel to the new Z axis:

$$\mathcal{H}_T = e^{i\theta I_y}\mathcal{H}_{er}e^{-i\theta I_y} \,. \tag{10}$$

After some trivial manipulations the Hamiltonian $\mathcal{H}_T$ in this tilted reference frame may be written as

$$\begin{aligned}\mathcal{H}_T = \hbar\{&-\langle\omega_e\rangle I_Z - \textstyle\sum_k[(\Delta\omega_{xz})_k I_{Zk}\cos(\theta - \theta_{xzk}) \\ &- (\Delta\omega_{xz})_k I_{Xk}\sin(\theta - \theta_{xzk}) + (\Delta\omega_{1y})_k I_{Yk}] \\ &+ \hat{\mathcal{H}}_c + \hat{\mathcal{H}}_d\},\end{aligned} \tag{11}$$

with

$$(\Delta\omega_{xz})_k=[(\Delta\omega_{oz})_k^2+(\Delta\omega_{1x})_k^2]^{1/2}\ , \tag{12}$$

$$\theta_{xzk}=\arctan\left|\ (\Delta\omega_{1x})_k/(\Delta\omega_{0z})_k\right|\ , \tag{13}$$

$$\hat{\mathcal{H}}_c=\textstyle\sum_i\ \delta_i\ (I_{Zi}\cos\theta-I_{Xi}\sin\theta)\ , \tag{14}$$

$$\hat{\mathcal{H}}_d=\sum_{M=-2}^{2}\lambda_M\ (\theta)\hat{\mathcal{H}}_M\ , \tag{15}$$

where the secular and nonsecular dipolar terms are those with $M=0$ and $M\neq 0$, respectively.

Under present experimental conditions, the first term of Eq. (11) is very large compared to any of the other terms. Therefore, within a first-order approximation, those terms of Eq. (11) which do not commute with I_Z can be dropped. Then $\mathcal{H}_T$ becomes

$$\mathcal{H}_T=\hbar[-\langle\omega_e\rangle I_Z+\hat{\mathcal{H}}_e+\hat{\mathcal{H}}_c'+\lambda_0\ (\theta)\hat{\mathcal{H}}_0]\ , \tag{16}$$

where

$$\hat{\mathcal{H}}_c'=\cos\theta\ \textstyle\sum_i\ \delta_i I_{Zi}\ , \tag{17}$$

$$\hat{\mathcal{H}}_e=-\textstyle\sum_k I_{Zk}(\Delta\omega_{xz})_k\cos(\theta-\theta_{xzk})\ , \tag{18}$$

$$\hat{\mathcal{H}}_0=\sum_{i<j}B_{ij}\ (I_{Zi}I_{Zj}-\tfrac{1}{3}\vec{\mathrm{I}}_i\cdot\vec{\mathrm{I}}_j),$$

and (19)

$$\lambda_0(\theta)=\tfrac{1}{2}(3\cos^2\theta-1).$$

Equation (16) permits the following conclusions:
(i) The chemical-shift term $\hat{\mathcal{H}}_c'$ is reduced by a factor of $\cos\theta$ as compared to the chemical shift in the laboratory frame. At exact resonance ($\theta=90°$), $\hat{\mathcal{H}}_c'=0$, i.e., the chemical shift cannot be observed and, hence, any exchange couplings between nonequivalent spins will also escape detection.

(ii) Near the magic angle where $\lambda_0\ (\theta)\approx 0$, the secular dipolar term in Eq. (16) becomes very small. In this case, the nonsecular terms play an important role in broadening the FID. Therefore, RSE's can only be observed when the inhomogeneity term $\hat{\mathcal{H}}_e$ is comparable or larger than the nonsecular dipolar terms at the magic angle.

(iii) $\hat{\mathcal{H}}_e$ formally commutes with all the terms of Eq. (16) except $\hat{\mathcal{H}}_0$. However, $\hat{\mathcal{H}}_0$ is a rather short-range interaction, while $\hat{\mathcal{H}}_e$ is a smoothly varying function over the entire space occupied by the sample. Therefore, it may be assumed to a very good approximation that $\hat{\mathcal{H}}_e$ commutes with $\hat{\mathcal{H}}_0$.

We rewrite Eq. (16) in the following way:

$$\mathcal{H}_T=\hbar(\mathcal{H}_A+\mathcal{H}_B)\ , \tag{20}$$

where

$$\mathcal{H}_A=-\langle\omega_e\rangle I_Z+\hat{\mathcal{H}}_e\ , \tag{21}$$

$$\mathcal{H}_B=\hat{\mathcal{H}}_c'+\lambda_0\ (\theta)\hat{\mathcal{H}}_0\ . \tag{22}$$

Suppose we measure $M_z(t)$ in the first rotating frame. Then the normalized magnetization is given by the correlation function

$$G(t)=\frac{M_z(t)}{M_z(0)}=\frac{\mathrm{Tr}[I_zU_{er}(t)I_zU_{er}^{\dagger}(t)]}{\mathrm{Tr}I_z^2}\ , \tag{23}$$

where $U_{er}(t)$ is the time-development operator in this frame. Since the trace is invariant under any unitary transformation, we transform the trace to the tilted frame using $S=e^{-i\theta I_y}$ and S^{-1}. Then

$$G(t)=\frac{1}{\mathrm{Tr}I_z^2}\ \mathrm{Tr}[(I_Z\cos\theta-I_X\sin\theta)\ U_T(t)\times(I_Z\cos\theta-I_X\sin\theta)\ U_T^{\dagger}(t)]\ , \tag{24}$$

where

$$U_T(t)=T\exp[-(i/\hbar)\textstyle\int_0^t\mathcal{H}_T(t')\ dt']\ . \tag{25}$$

Since $\mathcal{H}_T$ is time independent, the integration in Eq. (25) can be done disregarding the time-ordering operator T. Then

$$U_T(t)=e^{-(i/\hbar)\mathcal{H}_T t}\ . \tag{26}$$

If, at time $t=\tau$, the magnetization vectors are flipped by 180°, then at $t=2\tau$ the echo amplitude is given by [using Eqs. (20)–(26)]

$$E(2\tau)=(1/\mathrm{Tr}I_z^2)\ \mathrm{Tr}(I_ze^{-i(-\mathcal{H}_A+\tilde{\mathcal{H}}_B)\tau}e^{-i(\mathcal{H}_A+\mathcal{H}_B)\tau}\times I_ze^{i(\mathcal{H}_A+\mathcal{H}_B)\tau}e^{i(-\mathcal{H}_A+\tilde{\mathcal{H}}_B)\tau}), \tag{27}$$

where

$$I_z=I_Z\cos\theta-I_X\sin\theta\ , \tag{28}$$

$$-\mathcal{H}_A=R(\pi)\mathcal{H}_AR^{\dagger}(\pi)\ , \tag{29}$$

$$\tilde{\mathcal{H}}_B=R(\pi)\mathcal{H}_BR^{\dagger}(\pi)=-\hat{\mathcal{H}}_c'+\lambda_0(\theta)\hat{\mathcal{H}}_0\ . \tag{30}$$

$R(\pi)$ is a 180° rotation operator around any axis in the XY plane. Since $[\mathcal{H}_A,\mathcal{H}_B]\approx 0$ and $[\mathcal{H}_A,\tilde{\mathcal{H}}_B]\approx 0$ from (iii), Eq. (27) becomes

$$E(2\tau)=(1/\mathrm{Tr}I_z^2)\ \mathrm{Tr}(I_ze^{-\tilde{\mathcal{H}}_B\tau}e^{-i\mathcal{H}_B\tau}\ I_ze^{i\mathcal{H}_B\tau}e^{i\tilde{\mathcal{H}}_B\tau}). \tag{31}$$

Equation (31) clearly indicates the possibility of eliminating any magnetic field inhomogeneities of H_e by producing spin echoes in the rotating frame.

III. EXPERIMENTAL RESULTS AND DISCUSSION

A. Illustration of RSE Formation

The pulse sequence used in obtaining RSE's at the magic angle is shown in Fig. 1. A strong rf pulse of length 2τ was applied to the sample. At time $\tau'(\tau'\leq\tau)$ a strong dc magnetic field pulse of width determined by $\gamma H_e'\tau_{dc}=\pi$ was turned on along the direction of H_0. This sequence of pulses is followed by a 90° sampling pulse at time $2\tau+t_d$. The delay time t_d was chosen such that $T_2\ll t_d\ll T_1$.

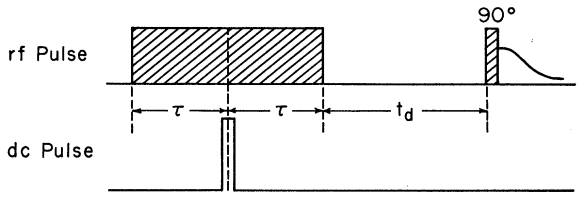

FIG. 1. Sequence of pulses producing RSE's at the magic angle ($T_2 \ll t_d \ll T_1$).

The amplitude of the ensuing FID then is a measure of the z component of magnetization, $M_z(2\tau)$, in the rotating frame[4,6,13] and was recorded as a function of the rf pulse length 2τ.

The formation of the RSE is illustrated in Fig. 2. (i) The equilibrium magnetization $M_z(0)$ initially aligned along $H_0\hat{z}$ in the first rotating frame precesses about $\vec{H}_e$, which is simply the vector sum of $(H_0 - \omega/\gamma)\hat{z}$ and $H_1\hat{x}$. $\omega/2\pi$ is the carrier frequency of the rf pulse. Under typical experimental conditions of $H_1 = 10$ G, the magic-angle condition $\cos\theta_m = \frac{1}{3}\sqrt{3}$ is realized by choosing $|H_0 - \omega/\gamma| = 5\sqrt{2}$ G. (ii) Because of the dominant H_e inhomogeneity, the magnetization will dephase distributing itself on a cone around H_e. (iii) When the dc field pulse is turned on along the direction of $-(H_0 - \omega/\gamma)\hat{z}$ at time τ', H_e changes instantly (within the rise time of the dc pulse) to a new effective field H_e'. The height of the dc pulse H_{dc} is adjusted such that $\vec{H}_e' \perp \vec{H}_e$. It is easily seen that H_{dc} should satisfy the condition $H_{dc} = 3|H_0 - \omega/\gamma|$. The dc pulse length τ_{dc} is adjusted such that the cone formed by the dephased magnetization is flipped by 180° around H_e'. (iv) After the dc pulse is turned off, the magic-angle condition is again satisfied but the fast and slow components of the magnetization are reversed while the sense of precession remains unchanged. (v) The dephased magnetization vectors will therefore be refocussed forming a rotary echo with location of its maxima at time $2\tau'$.

B. Preliminary Experiment Using Liquid Sample

The degree of refocussing the dephased magnetization at the magic angle was tested for the proton resonance in glycerine in which the interaction of the nuclear moments with the inhomogeneous H_e field completely dominates all other couplings. Since $T_2 \approx T_1 \approx 50$ msec, a dc field inhomogeneity was deliberately introduced to shorten the FID following the rf pulse such that any T_1 process was entirely negligible at the time of the application of the sampling pulse.

The detected signal $M_z(t)$ consists of a decaying oscillation of frequency ω_e superimposed on a constant term $M_z(0)\cos^2\theta$. Figure 3 shows the normalized envelope $K(t)$ of the signal defined by[6]

$$K(t) = \tfrac{1}{2}[(\text{upper envelope}) - (\text{lower envelope})], \quad (32)$$

where $K(t)$ represents the amplitude of the oscillatory part and is independent of the upward shift of the relaxation pattern by a constant amount which occurs for angles other than $\theta = 90°$. The dc pulse was applied at $t = \tau' = 2$ msec. The amplitude of the spin echo in the laboratory frame obtained by using a $90° \sim\tau\sim 180°$ pulse sequence with $\tau = 2$ msec recovers about 94% of the initial equilibrium magnetization. Assuming that all interactions in the sample are the same in the rotating frame and the laboratory frame, it can be concluded that the present technique recovers 99% of the transverse magnetization dephased under the action of the H_e inhomogeneity.

C. RSE's in Teflon

The F^{19} resonance in Teflon at 45 MHz has been studied for reasons of demonstrating the effectiveness of the RSE technique in solids. At room temperature its characteristic relaxation times are $T_2 \approx 33$ μsec and $T_1 \approx 25$ msec. The rf inhomogeneity ΔH_1 across the sample varied linearly with H_1 and amounted to about 2% of H_1.

Figure 4 shows a single RSE in Teflon at the

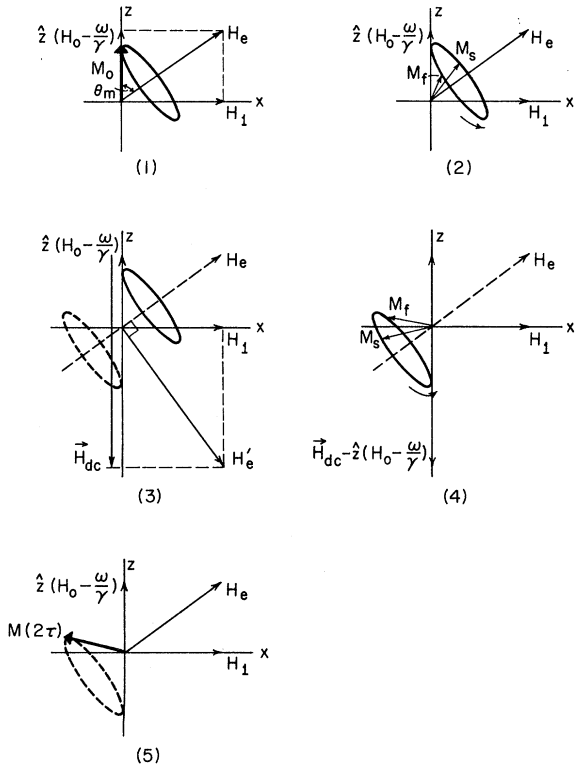

FIG. 2. Illustration of the refocussing process of the transverse magnetization at the magic angle in the rotating frame.

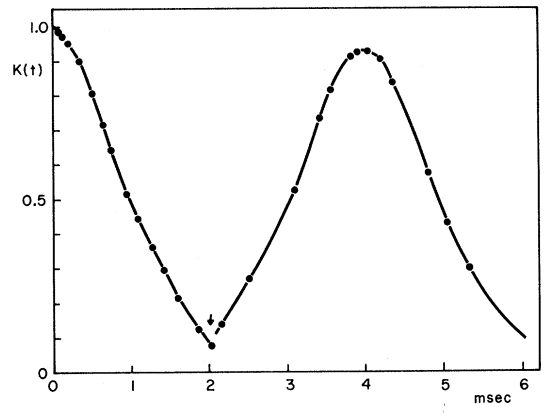

FIG. 3. Rotary FID envelope $K(t)$ at the magic angle showing a RSE in a liquid glycerine sample. Arrow indicates the position of the dc pulse.

magic angle. The circles indicate the experimental points corresponding to maxima and minima of the oscillating z component of magnetization. The initial $M_z(t)$ decay was obtained without applying the dc field pulse for reasons of comparison. A dc pulse was applied at $t=\tau'$ and the echo envelope was observed by changing the rf pulse length. H_1 used in taking this data was 8.4 G. The upward shift of the relaxation pattern with respect to the base line is due to the component of magnetization along H_e, i.e., $M_z(0)\cos^2\theta_m = \frac{1}{3}M_z(0)$, which decays with the characteristic time $T_{1\rho}$, the longitudinal relaxation time in the rotating frame. The narrowing of the line is, of course, independent of this shift and completely described by $K(t)$ defined by (32).

It is evident from Fig. 4 that only part of the transverse magnetization could be recovered. In addition, a shift of the echo maximum to the left is noticeable. These observations indicate that effects other than the H_e inhomogeneity limit the lifetime of the narrowed FID, such as nonsecular dipolar terms or second-order inhomogeneity broadening. The latter were neglected in the calculation and arise because H_e itself may be spread over a cone rather than being represented by a single vector.

In order to trace out the complete decay of the signal in the rotating frame while eliminating rf inhomogeneity broadening, τ' was varied from 20 to about 500 μsec in steps of 20 μsec and the resulting RSE envelopes around their respective position at $t=2\tau'$ were recorded. All these envelopes were smoothly connected. The normalized function $K(t)$ is shown in Fig. 5 and is compared with the FID in the laboratory frame. For large t, the RSE envelope decays exponentially. Defining a transverse relaxation time $T_{2\rho}$ in the rotating frame as the time constant of the exponential part of the function $K(t)$, i.e.,

$$\lim_{t\to\infty} K(t) = K_0\, e^{-t/T_{2\rho}} \quad (t \ll T_{1\rho}) \,, \tag{33}$$

one obtains $T_{2\rho}\approx 603$ μsec. This value has to be corrected by the contribution of the longitudinal relaxation with time constant $T_{1\rho}\approx 5.3$ msec for $H_1 = 8.4$ G (from Fig. 9). One then obtains a time constant of about 680 μsec. Applying definition (33) to the laboratory FID yields $T_2 \approx 33$ μsec. Hence, the fluorine resonance has been narrowed by about a factor of 20. Estimates indicate that the decay is primarily caused by nonsecular dipolar terms rather than any second-order inhomogeneity effects.[6] H_1 should therefore be increased further to achieve more spectacular line narrowings.

The RSE in Fig. 6 was obtained under conditions identical to the previous data except that the inhomogeneity of the static field H_0 was increased drastically. The initial envelope decays faster as compared to that of Fig. 4. As a result, the observed echo envelope is more clearly distinguished. In spite of the additional H_0 inhomogeneity, the magnetization at $t=2\tau'$ is recovered to the extent possible in applying a continuous rf field of 8.4 G to this compound.

An obvious generalization of the present procedure consists of the application of many dc field pulse inversions of the fast and slow components of the decaying magnetization in the rotating frame. Such a technique would correspond to a Carr-Purcell sequence in the laboratory frame. Figure 7 shows the decay and subsequent recovery of the magnetization in Teflon under the action of two dc field pulses. Again, the time constant of the RSE envelope agrees with the previous results within experimental accuracy.

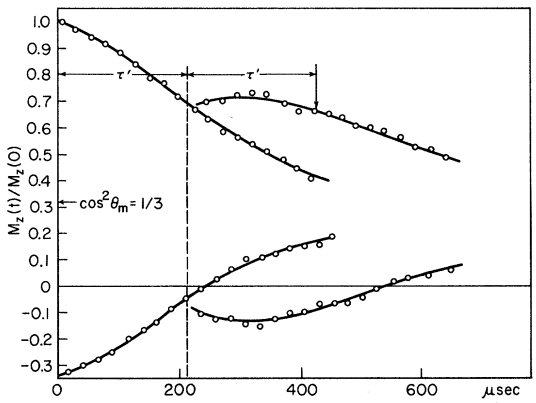

FIG. 4. RSE in Teflon. Circles represent the experimentally observed maximum and minimum values of $M_z(t)$. $H_1 = 8.4$ G.

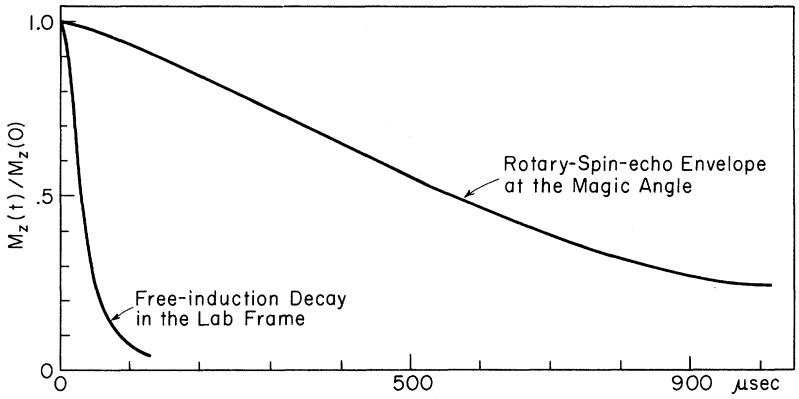

FIG. 5. Normalized RSE envelope for Teflon at the magic angle ($H_1 = 8.4$ G). FID following a 90° pulse is plotted for comparison.

D. Measurement of $T_{1\rho}$ in Teflon

The spin-lock technique[14] was used in measuring the longitudinal relaxation time $T_{1\rho}(\theta, H_1)$ as a function of H_1 at exact resonance ($\theta = 90°$), and as a function of θ for two fixed H_1 values. A 90° pulse was immediately followed by a 90° phase-shifted long rf pulse of variable width. The amplitude of the signal following the second rf pulse was recorded as a function of its pulse length. The signal amplitude so obtained showed a purely exponential decay from which $T_{1\rho}$ was extracted.

The variation of $T_{1\rho}(90°)$ with H_1 is plotted in Fig. 8. It is approximately linear within the range of H_1 values used. $T_{1\rho}$ should approach T_1 for large H_1. Johnson and Goldburg have measured $T_{1\rho}(90°)$ in a single crystal of NaCl as a function of H_1.[15] Their results show that $T_{1\rho} \approx T_1$ for H_1 above 5 G. The values of $T_{1\rho}(90°)$ in Teflon for H_1 of up to 12 G, however, are quite small as compared to T_1 ≈250 msec. This result can only be understood if the F^{19} spin-lattice relaxation at room temperature is dominated by slow motional effects such as hindered rotation or atomic diffusion. Within the restriction of the range of applied H_1 amplitudes it then appears that the correlation time τ_c of the motion must be semicontinuous in the range of a few μsec. Of course, this statement is somewhat speculative as it is based on measurements at only one temperature. However, the following results seem to confirm this conclusion, at least qualitatively.

Figure 9 shows $T_{1\rho}(\theta, H_1)$ as a function of θ for H_1 values of 5.91 and 9.75 G, respectively. Particular care was given to measurements near the magic angle ($\theta = 54.7°$). No discontinuity of the $T_{1\rho}$'s was found, indicating that any contribution of spin diffusion to the longitudinal relaxation of the F^{19} spins is negligible.[8] Jones[16] has calculated $T_{1\rho}(\theta)$ in the rotating frame including all dipolar terms. He assumed an isotropic random motion of the spins with a single correlation time τ_c characterizing the motion. His result for spin $-\frac{1}{2}$ nuclei is given by

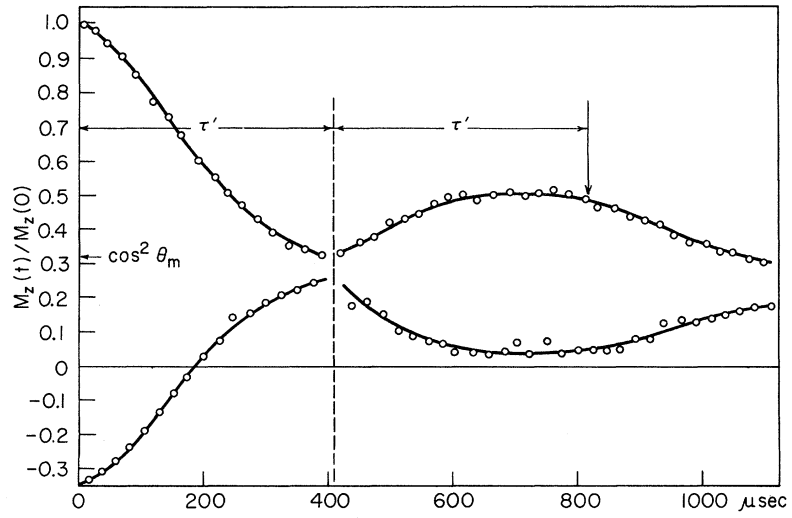

FIG. 6. RSE in Teflon obtained in a strongly inhomogeneous dc magnetic field. $H_1 = 8.4$ G.

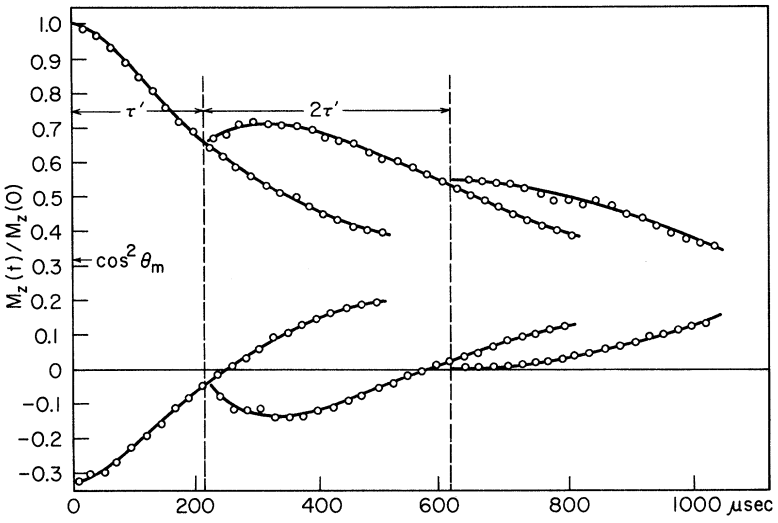

FIG. 7. RSE's in Teflon obtained under the action of two successive dc field pulses at τ' and $2\tau'$. $H_1 = 8.4$ G.

$$\frac{1}{T_{1\rho}} = K\tau_c\left(\tfrac{3}{2}\sin^2\theta + \frac{1+\frac{3}{2}\sin^2\theta}{1+\omega_0^2\tau_c^2} + \frac{4-3\sin^2\theta}{1+4\omega_0^2\tau_c^2}\right), \tag{34}$$

where K is a constant. Although this model applies only partially to Teflon, K and τ_c can be formally determined from any two values of $T_{1\rho}$[e.g., $T_{1\rho}(90°)$ and $T_{1\rho}(0°) = T_1$]. The solid curves in Fig. 9 were drawn to match the experimental results yielding the values of $K\tau_c = 493.56$ sec^{-1} and $\tau_c = 2.12$ μsec. The latter is of the same order of magnitude as the values of τ_c estimated from Fig. 8.

IV. SUMMARY

The method of narrowing dipolar broadened lines in solids by means of irradiating the sample with strong continuous rf fields has been improved by generating RSE's. When H_e is larger than the local field, any H_e inhomogeneity broadening can be eliminated in first order. Any second-order inhomogeneity effects should be quite small under present experimental conditions but may become nonnegligible and, indeed, the dominant source of broadening once the dipolar coupling is completely truncated in the tilted rotating frame. Line narrowing of up to a factor of 20 could be obtained in Teflon.

It is evident from the results that even higher H_1 amplitudes are required to eliminate all contributions from the nonsecular dipolar terms. These will

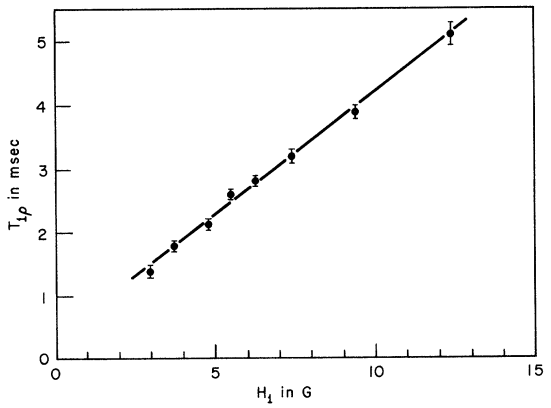

FIG. 8. $T_{1\rho}(90°)$ in Teflon as a function of H_1.

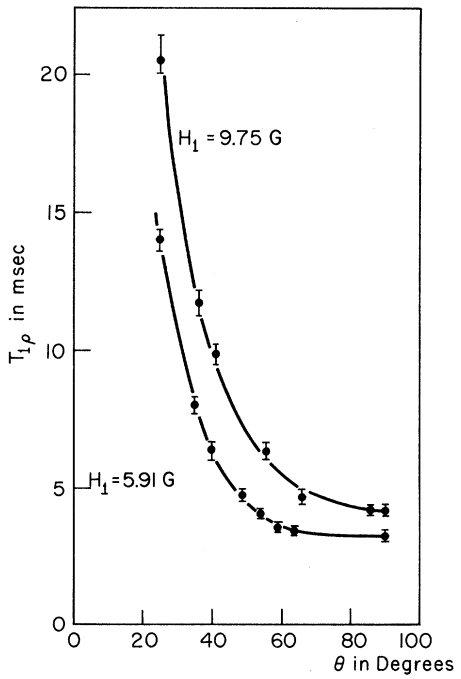

FIG. 9. $T_{1\rho}(\theta)$ in Teflon as a function of θ for two values of H_1. Solid line is obtained from theory [Eq. (34)].

have to be matched by more intense dc field pulses with short rise and fall times for off-resonance observations. From this point of view the choice of Teflon appears to be a rather poor one since the nonsecular terms in this compound are surprisingly large in the range of rf fields used. As compared to sample rotation and multiple-pulse-sequence techniques the continuous rotating field approach has the disadvantage that the signal is not observable in the presence of the rf field.

*Work supported by the University of North Carolina Materials Research Center under Contract No. SD-100 from the Advanced Research Projects Agency.

†Now at the Department of Chemistry and Research Laboratory of Electronics, Massachusetts Institute of Technology, Cambridge, Mass. 02139.

[1]A summary of the literature concerned with sample rotation has been given by E. R. Andrew, in *Magnetic Resonance*, edited by C. K. Coogan *et al.* (Plenum, New York, 1970).

[2]N. Bloembergen, E. M. Purcell, and R. V. Pound, Phys. Rev. 73, 679 (1948).

[3]A. G. Redfield, Phys. Rev. 98, 1787 (1955).

[4]W. I. Goldburg and M. Lee, Phys. Rev. Letters 11, 255 (1963).

[5]D. Barnaal and I. J. Lowe, Phys. Rev. Letters 11, 258 (1963).

[6]M. Lee and W. I. Goldburg, Phys. Rev. 140, A1261 (1965).

[7]U. Haeberlen and J. S. Waugh, Phys. Rev. 175, 453 (1968), and previous references cited therein.

[8]H. Kessemeier and R. E. Norberg, Phys. Rev. 155, 321 (1967).

[9]E. R. Andrew, L. F. Farnell, and T. D. Gledhill, Phys. Rev. Letters 19, 6 (1967).

[10]J. S. Waugh and L. M. Huber, J. Chem. Phys. 47, 1862 (1967).

[11]P. Mansfield and K. H. B. Richards, Chem. Phys. Letters 3, 169 (1969).

[12]W. A. B. Evans, Ann. Phys. (N. Y.) 48, 72 (1968).

[13]W. K. Rhim and H. Kessemeier, Phys. Rev. B 3, 3655 (1971).

[14]S. R. Hartmann and E. L. Hahn, Phys. Rev. 128, 2042 (1962).

[15]B. C. Johnson and W. I. Goldburg, Phys. Rev. 145, 380 (1966).

[16]G. P. Jones, Phys. Rev. 148, 332 (1966).

PHYSICAL REVIEW B VOLUME 5, NUMBER 3 1 FEBRUARY 1972

Energy Distribution in Field Emission from Adsorbate-Covered Surfaces*

D. Penn,† R. Gomer, and M. H. Cohen
The James Franck Institute, The University of Chicago, Chicago, Illinois 60637

(Received 21 June 1971)

A calculation of the total energy distribution of field-emitted electrons in the presence of chemisorbed atoms shows that $[j(\omega)-j_0(\omega)]/j_0(\omega)=u(\omega)^2\ \mathrm{Im}G_{aa}(\omega)$ if the adsorbate resonance level lies within the conduction band of the metal. $j(\omega)$ and $j_0(\omega)$ are the current densities per unit energy in the presence and absence of the adsorbate, respectively; the energy ω is measured from the vacuum level; x_a is the surface-adsorbate distance; and $(1/\pi)\ \mathrm{Im}G_{aa}$ is the local density of states at the adsorbate. $u(\omega)^2\propto\exp\{2(-2m\omega/\hbar^2)^{1/2}x_a+[\frac{4}{3}(2m/\hbar^2)^{1/2}(-\omega)^{3/2}(eF)^{-1}\times(v(y)-1)]\}$, where F is the electric field and $v(y)$ is the image-potential correction factor. The expression given above for the tunneling current is general and independent of the explicit form of G_{aa}. If the adsorbate resonance lies below the bottom of the conduction band, then $[j(\omega)-j_0(\omega)]/j_0(\omega)<0$, in agreement with the results of Duke and Alferieff.

I. INTRODUCTION

Measurements of total energy distribution (TED) of field-emitted electrons from adsorbate-covered surfaces can show the location and shapes of the virtual impurity levels associated with the adsorbate, and thus constitute a powerful tool for the study of chemisorption. Theoretical treatments of tunneling through adsorbates have been given by Duke and Alferieff[1] (DA) and by Gadzuk.[2] Both DA and Gadzuk formulated the problem in terms of tunneling of metal electrons through an adsorbate schematized in terms of a potential. DA considered only one-dimensional cases, and their parametrization does not easily lend itself to interpretations of specific systems nor does it take correlation effects into account. Gadzuk has attempted to attack the problem specifically from the point of view of obtaining information on virtual adsorbate levels. However, it is hard to see the justification for his initial state function $|m\rangle+GV_F|m\rangle$ used in Eq. (8) of his paper and central to his subsequent development, since G is the Green's function appropriate to the total field-free Hamiltonian, metal plus adsorbate, while $|m\rangle$ is an eigenfunction of the metal Hamiltonian only, and V_F, the external electric field, is in this context a higher-order perturbation. In the case of chemisorption, however, the